

# RecBCD Enzyme Switches Lead Motor Subunits in Response to $\chi$ Recognition

Maria Spies,<sup>1,3</sup> Ichiro Amitani,<sup>1</sup> Ronald J. Baskin,<sup>2</sup> and Stephen C. Kowalczykowski<sup>1,2,\*</sup>

<sup>1</sup>Section of Microbiology

<sup>2</sup>Section of Molecular and Cellular Biology

University of California, Davis, CA 95616-8665, USA

<sup>3</sup>Department of Biochemistry, University of Illinois at Urbana-Champaign, Urbana, IL 61801-3602, USA

\*Correspondence: sckowalczykowski@ucdavis.edu

DOI 10.1016/j.cell.2007.09.023

## SUMMARY

RecBCD is a DNA helicase comprising two motor subunits, RecB and RecD. Recognition of the recombination hotspot,  $\chi$ , causes RecBCD to pause and reduce translocation speed. To understand this control of translocation, we used single-molecule visualization to compare RecBCD to the RecBCD<sup>K177Q</sup> mutant with a defective RecD motor. RecBCD<sup>K177Q</sup> paused at  $\chi$  but did not change its translocation velocity. RecBCD<sup>K177Q</sup> translocated at the same rate as the wild-type post- $\chi$  enzyme, implicating RecB as the lead motor after  $\chi$ . P1 nuclease treatment eliminated the wild-type enzyme's velocity changes, revealing a  $\chi$ -containing ssDNA loop preceding  $\chi$  recognition and showing that RecD is the faster motor before  $\chi$ . We conclude that before  $\chi$ , RecD is the lead motor but after  $\chi$ , the slower RecB motor leads, implying a switch in motors at  $\chi$ . We suggest that degradation of foreign DNA needs fast translocation, whereas DNA repair uses slower translocation to coordinate RecA loading onto ssDNA.

## INTRODUCTION

The RecBCD helicase/nuclease is needed for recombinational DNA repair of double-stranded DNA (dsDNA) breaks in *E. coli* (for review see Spies and Kowalczykowski, 2005). To initiate repair, RecBCD binds to the broken duplex DNA end, unwinds the dsDNA for 30 kb on average, and differentially degrades both nascent DNA strands. While translocating, RecBCD can recognize a specific DNA sequence,  $\chi$  (Chi, crossover hotspot instigator; 5'-G CTGGTGG-3'), which is a hotspot for homologous recombination (Lam et al., 1974). Recognition of  $\chi$  attenuates the nuclease activity of the enzyme (Anderson and Kowalczykowski, 1997a; Dixon and Kowalczykowski, 1991, 1993), resulting in production of a long single-stranded DNA (ssDNA) tail with the  $\chi$  sequence at its 3' end. RecBCD facilitates loading of the DNA strand exchange protein,

RecA, onto this  $\chi$ -containing ssDNA to form the RecA nucleoprotein filament that acts subsequently to promote homologous pairing of DNA (Anderson and Kowalczykowski, 1997b). In addition to regulating nucleolytic and RecA-loading activities,  $\chi$  recognition regulates translocation behavior: RecBCD pauses at  $\chi$  for several seconds and subsequently reduces its translocation velocity (Spies et al., 2003). The manner by which  $\chi$  effects these changes in movement is unknown. RecBCD employs two autonomous motor subunits, RecB and RecD, that translocate on opposite strands of the DNA duplex (Dillingham et al., 2003; Taylor and Smith, 2003), so we imagined that the  $\chi$ -induced changes in translocation are mediated through one or both of these motor subunits.

Previously, we proposed two models to explain the translocation pause and velocity change elicited by  $\chi$  recognition (Spies et al., 2003). One model posited that the two motor subunits of RecBCD translocate along their respective DNA strands at different rates; in this model, translocation by the motors is *uncoupled*. Thus, the faster motor would be the "helicase" subunit responsible for strand separation, and the slower motor subunit would be a "translocase" simply translocating along the ssDNA produced by the lead motor. In this model, the unequal translocation rates of two motors would produce a loop of ssDNA between the fast motor and slow motor (Figure 1A). We proposed that when RecBCD recognizes  $\chi$ , the lead motor subunit stops translocating at or near  $\chi$ , resulting in the pause. However, the slower motor continues translocating along its ssDNA track until it catches up to the other paused motor subunit at  $\chi$ . It then becomes the "helicase" motor of the enzyme.

The alternative model (Figure 1B) proposed that two motor subunits translocate coordinately at the same velocity before  $\chi$ ; in this model, translocation by the motors is *concerted*. Cooperation of two motors was envisioned as being responsible for the fast enzyme translocation. The pause at  $\chi$  was attributed to the time required for a  $\chi$ -induced conformational change. In this model, the reduced rate after  $\chi$  is a consequence of inactivation of one of the motors. Thus, in this second model, two motors operate in concerted fashion as the helicase before  $\chi$ , but only one motor functions after  $\chi$ .

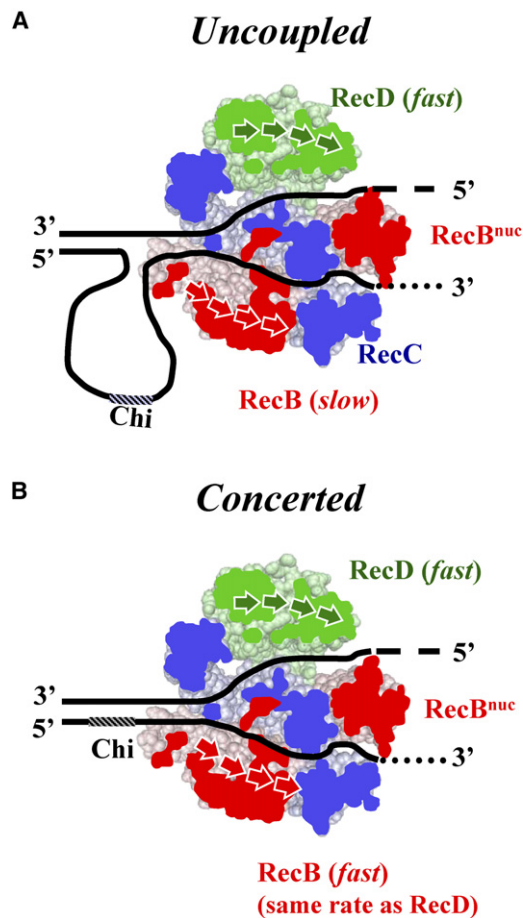


**Figure 1. Models of Uncoupled versus Concerted Translocation by RecBCD prior to  $\chi$  Recognition**

(A) In the “Uncoupled” translocation model, the two motor subunits, RecB and RecD, can translocate independently of one another. In the illustration, RecD is shown as the faster lead motor subunit and RecB as the slower motor; faster translocation by RecD will result in accumulation of ssDNA originating from the 3'-terminated strand in front of RecB.

(B) In the “Concerted” translocation model, the two motor subunits translocate at equal speeds and work coordinately to move the enzyme. Arrows indicate the directions that ssDNA moves through the motors.

Existing data could be mustered in support of either model. In our previous single-molecule experiments, we found that the duration of the pause was not simply related to the difference in time needed by each motor to travel to  $\chi$ , based on the rates of the putative fast and slow subunits before and after  $\chi$ , respectively (Handa et al., 2005; Spies et al., 2003). This finding was inconsistent with the simplest version of the uncoupled motors model and, therefore, pointed toward the concerted motors model. However, the uncoupled motors model was consistent with the existence of the loop-tail unwinding intermediates that were observed prior to  $\chi$  recognition by electron microscopy (Taylor and Smith, 1980, 2003). On the other hand, the behavior of mutant enzymes defective in one

or the other motor subunit showed that the dual motor holoenzyme was a faster and more processive helicase than either mutant, which showed that the holoenzyme was more than its constituent parts, and which was consistent with the concerted motors model (Dillingham et al., 2005; Spies et al., 2005).

Analysis of the mutant RecBCD enzymes, RecB<sup>K29Q</sup>CD and RecBCD<sup>K177Q</sup>, wherein the motor functions of RecB and RecD, respectively, were inactivated by mutagenesis (Dillingham et al., 2005; Spies et al., 2005), revealed that a functional RecB motor is required for  $\chi$  recognition in vitro and for recombination function in vivo. In contrast, the RecD motor is virtually dispensable, although it did endow the enzyme with increased translocation speed and greater processivity. In contrast to the RecB<sup>K29Q</sup>CD mutant, RecBCD<sup>K177Q</sup> could recognize and respond to a recombination hotspot  $\chi$  (Spies et al., 2005). Consequently, here we analyzed the translocation behavior of just the RecBCD<sup>K177Q</sup> both before and after an encounter with  $\chi$ . Because of the intrinsic heterogeneity in translocation velocities manifest by an ensemble of RecBCD enzymes, the only means for detecting the pause and velocity change at  $\chi$  is the single-molecule assay that we described previously (Bianco et al., 2001; Handa et al., 2005; Spies et al., 2003).

Here we use optical trapping of single DNA-RecBCD complexes to characterize translocation by individual wild-type and mutant RecBCD<sup>K177Q</sup> enzymes on  $\chi$ -containing DNA substrates. Our findings show that  $\chi$  recognition by the RecBCD results in an unanticipated switch in motor usage at  $\chi$ : prior to  $\chi$ , RecD is the lead motor, but after  $\chi$ , RecB becomes the lead motor.

## RESULTS

### RecBCD<sup>K177Q</sup> Pauses at $\chi$ but Does Not Alter Its Translocation Rate after $\chi$ Recognition

To determine whether the function of both motor subunits is required for the  $\chi$ -induced pause and change in translocation rate by RecBCD, we analyzed translocation of individual RecBCD<sup>K177Q</sup> mutant enzymes. In this mutant, a lysine-to-glutamine substitution in the Walker A motif inactivates ATP binding by the RecD subunit and abolishes its ability to translocate along ssDNA (Korany and Julin, 1992), leaving the RecB subunit as the only functional motor in this enzyme. For these measurements, we designed a DNA substrate in which a correctly oriented  $\chi$  locus was positioned 5.26 kb from the free DNA end. The substrate is schematically shown to the right of the graph in Figure 2. Figure 2 also shows a representative time trace for translocation by the wild-type RecBCD (blue points and line). As we showed previously (Spies et al., 2003), the wild-type enzyme paused (4.6 s for the molecule in Figure 2) in response to  $\chi$  recognition and then reduced its translocation rate (2.9-fold for this molecule). Analysis of 22 RecBCD molecules (summarized in Table 1) showed that the average velocity of translocation for the wild-type enzyme before  $\chi$  was approximately

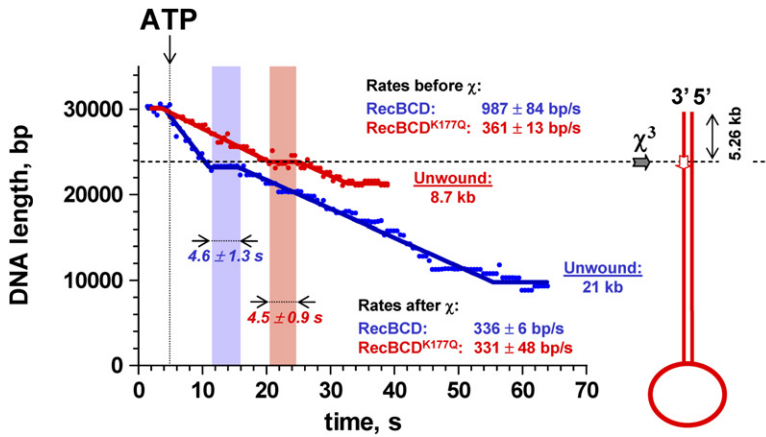


**Figure 2. The RecD Motor-Defective Mutant, RecBCD<sup>K177Q</sup>, Pauses at  $\chi$  but Does Not Alter Its Translocation Velocity after  $\chi$  Recognition**

Time courses for DNA unwinding of a single DNA molecule containing  $\chi$  positioned 5.26 kb from the DNA end. The DNA substrate is shown schematically on the right. The arrow above the graph shows when the RecBCD-DNA-bead complex was moved into the ATP-containing channel. The length of the DNA molecule was measured for each frame of a video and is plotted as a function of time for RecBCD (blue circles) and RecBCD<sup>K177Q</sup> (red circles). The rates of DNA unwinding and both the duration and the position of the pause were determined by fitting the data to a continuous 5 segment line (the fitted lines for wild-type and mutant are shown in blue and red, respectively). Blue and red shaded rectangles indicate the respective periods when RecBCD and RecBCD<sup>K177Q</sup> are paused. The extent of DNA unwinding is indicated.

2-fold greater than after  $\chi$ . As reported previously, both the translocation velocity and the change in velocity for individual enzymes varied greatly (Figures 3A and 3C). Also as previously reported (Spies et al., 2003), the translocation velocity of each wild-type enzyme before  $\chi$  is always greater, within experimental error, than its velocity after  $\chi$  (Figure 3A). Furthermore, there is no correlation between the translocation velocity prior to  $\chi$  and the velocity after  $\chi$ , illustrating not only the intrinsic heterogeneity, but

also suggesting that different motor forms of the enzyme might be responsible for translocation before and after  $\chi$ .

In comparison to the wild-type, the behavior of RecBCD<sup>K177Q</sup> is different (Figure 2, red circles and line). Although the frequency of  $\chi$  recognition for RecBCD<sup>K177Q</sup> was similar to that of the wild-type (Table 1), the trajectory shows that, even though this mutant enzyme pauses at  $\chi$  for 4.5 s, it does not change its translocation velocity beyond  $\chi$ . The mutant RecBCD<sup>K177Q</sup> contains only one

**Table 1. Summary of Parameters for the Unwinding of  $\chi$ -Containing dsDNA by Wild-Type RecBCD and RecBCD<sup>K177Q</sup> Enzymes**

	RecBCD	RecBCD + P1 Nuclease	RecBCD <sup>K177Q</sup>	RecBCD <sup>K177Q</sup> + P1 Nuclease
DNA molecules analyzed	26	28	26	14
Unwinding detected	22	23	21	12
Rate before $\chi$ , bp/s	$629 \pm 368$	$609 \pm 274$	$333 \pm 133$	$415 \pm 51$
Rate after $\chi$ , bp/s	$379 \pm 124$	N/A	$324 \pm 163$	$402 \pm 99$
Frequency of $\chi$ recognition <sup>a</sup>	52%	N/A	40%	33%
Pause half-life (s)	$3.5 \pm 0.3$	no pause	$3.9 \pm 0.2$	$3.2 \pm 0.3$
Position of the pause (kb)	$5.8 \pm 1.3$	no pause	$5.4 \pm 0.6$	$5.2 \pm 1.1$
Processivity <sup>b</sup> (N, kb)	$0.999945 \pm 0.000002$ (18.2)	$0.999926 \pm 0.000003$ (13.5)	$0.99978 \pm 0.00007$ (4.5)	$0.99978 \pm 0.00007$ (4.5)

Values for the rates and both the position and duration of the pauses are given as an average value for all molecules  $\pm$  one standard deviation unit.

<sup>a</sup> The frequency of  $\chi$  recognition is expressed per  $\chi$  sequence.

<sup>b</sup> Processivity was calculated by plotting the number of enzymes (Y) that unwound at least a given DNA length (grouped in 1 kb bins) versus that length (X). Processivity, P, was determined by fitting the data to the equation  $Y = A \cdot P^X$ . The average extent of unwinding, N, was obtained from P by the equation  $N = 1/(1 - P)$ . We note that the processivity for wild-type is lower than previous reports (Bianco et al., 2001; Handa et al., 2005; Roman et al., 1992), we suspect, because of imperfections in the DNA substrates that are introduced by PCR.

functional motor, so the observation of a pause eliminates the possibility that pausing by the wild-type RecBCD stems solely from the difference in the translocation rates for the two motors. Interestingly, the distribution of pause times is clearly exponential, suggesting that the pause time reflects a dwell time or kinetic lifetime (Figure 3E). More interestingly, the exponential distributions of the pauses for the wild-type and mutant enzymes yield identical lifetimes (within error) of 3.5 ( $\pm 0.3$ ) and 3.9 ( $\pm 0.2$ ) s, respectively (Table 1). Furthermore, the pause times at  $\chi$  loci located approximately 7 and 8 kb from the DNA end, which we reported earlier (Spies et al., 2003), each also display an exponential distribution with an identical lifetime (data not shown). Consequently, we now conclude that the pause can be attributed to a lifetime associated with  $\chi$  binding and that this lifetime likely reflects the time needed for the conformational change that occurs in response to  $\chi$  recognition.

In contrast to wild-type, the RecBCD<sup>K177Q</sup> mutant shows no change in the translocation velocity upon  $\chi$  recognition: both the mean and distribution of translocation velocities before and after pausing at  $\chi$  were the same within experimental error (333 [ $\pm 133$ ] versus 324 [ $\pm 163$ ]) (Figure 3D and Table 1). Furthermore, for each RecBCD<sup>K177Q</sup> that paused at  $\chi$ , the translocation velocity after the pause was identical to that before  $\chi$ , within error (Figure 3B). These data indicate that the fast translocation behavior prior to  $\chi$  requires a functioning RecD motor subunit. Suggestively, both the mean and the distribution of translocation rates for both RecBCD<sup>K177Q</sup> and the post- $\chi$  state of the wild-type enzyme ( $\chi$ -modified) were similar: 324 ( $\pm 163$ ) bp/s and 379 ( $\pm 124$ ) bp/s (Table 1; Figures 3C and 3D), insinuating that the RecB motor drives the  $\chi$ -modified enzyme. Thus, the most economical conclusion from these results is that RecB subunit is both the lead motor and helicase subunit after  $\chi$ . However, these findings do not address the question of whether the faster translocation seen prior to  $\chi$  for the wild-type enzyme is due to RecB and RecD acting in a concerted manner or to either RecB or RecD being the faster of a pair of uncoupled motors.

### P1 Nuclease Treatment Eliminates Both the Pause and Change in Translocation Velocity of the RecBCD that Is Elicited by $\chi$ Recognition

In the uncoupled motors model, if one of the subunits is the lead motor that is responsible for DNA unwinding prior to  $\chi$  and the other subunit is the slower motor that lags behind translocating along the ssDNA, then the wild-type enzyme should generate a ssDNA loop that grows with distance. Indeed, such structures have been observed by electron microscopy and have revealed that the RecD subunit is the lead motor under those conditions (Braedt and Smith, 1989; Muskavitch and Linn, 1982; Taylor and Smith, 1980, 2003). However, given that the kinetic parameters for DNA unwinding by RecB and RecD are significantly affected by solution conditions (e.g., concentrations of ATP and divalent metal ions [Dillingham et al., 2005; Spies et al., 2005]), we sought to independently

determine whether RecD was the faster subunit under our reaction conditions. If, as depicted in Figure 1A, RecD is the faster motor subunit, then the expected ssDNA loop would be in front of the RecB subunit on the DNA strand that contains the  $\chi$  sequence; in contrast, if RecB were the faster motor, then the converse would be true. Consequently, these two scenarios can be distinguished by determining whether  $\chi$  is ever revealed as ssDNA in the presumptive loop. The case of RecD being the faster subunit is unique because, if the ssDNA in the loop could be continually degraded by an exogenous ssDNA-specific endonuclease (Figure 4B), then there would be no  $\chi$  sequence to recognize; hence, both the pause and the change in the translocation velocity should be eliminated. However, if the two motor subunits translocated at the same rate before  $\chi$  (the concerted translocation model in Figure 1B) or if RecB were the faster motor prior to  $\chi$ , then no ssDNA loop would form on the  $\chi$ -containing strand, and consequently, an ssDNA-specific nuclease would not interfere with the  $\chi$ -induced pause and change in the translocation rate. To discriminate between the two models, we added the ssDNA-specific endo/exonuclease, P1, to the reaction channel of the flow cell.

In the presence of P1 nuclease, the translocation behavior of RecBCD prior to  $\chi$  was unaffected (Figure 4A, blue circles and line; Table 1). However, in stark contrast, P1 nuclease completely eliminated  $\chi$  recognition, as manifested by both the pause and the velocity change. All of the wild-type RecBCD enzymes ( $n = 19$ ) that translocated beyond  $\chi$  failed to respond to  $\chi$  in the presence of P1 nuclease. These data support our inference and the prior EM observations (Taylor and Smith, 2003) that a loop of ssDNA is formed between the two motor subunits. This loop forms on the 3'-terminal DNA strand that contains the  $\chi$  sequence and is the strand along which the RecB subunit translocates. Hence, RecD is the faster motor subunit prior to  $\chi$ .

### P1 Nuclease Activity Does Not Interfere with $\chi$ Recognition by the RecBCD<sup>K177Q</sup> Mutant

To eliminate the possibility that P1 nuclease was acting nonspecifically to block  $\chi$  recognition by RecBCD, we also tested its effect on RecBCD<sup>K177Q</sup>. Because RecB is the only motor subunit of RecBCD<sup>K177Q</sup>, a loop cannot form on the  $\chi$ -containing strand. Therefore, if P1 nuclease were blocking  $\chi$  recognition by degrading the hypothesized ssDNA loop that contains the  $\chi$  sequence, then P1 nuclease should have no effect on this mutant enzyme. When an identical amount of P1 nuclease was used, the RecBCD<sup>K177Q</sup> mutant enzyme was completely unaffected by its presence (Figure 4A, red circles and line). A representative time trace for translocation by the RecBCD<sup>K177Q</sup> in the presence of P1 nuclease (Figure 4A, red circles) clearly shows that this single-motor enzyme pauses at  $\chi$  and then continues translocating at a similar rate. Both the average duration of the pause (Figure 3B) and the translocation rate before and after  $\chi$  (Table 1) were similar to those observed in the absence of nuclease, confirming that RecBCD<sup>K177Q</sup>, whose translocation is supported by



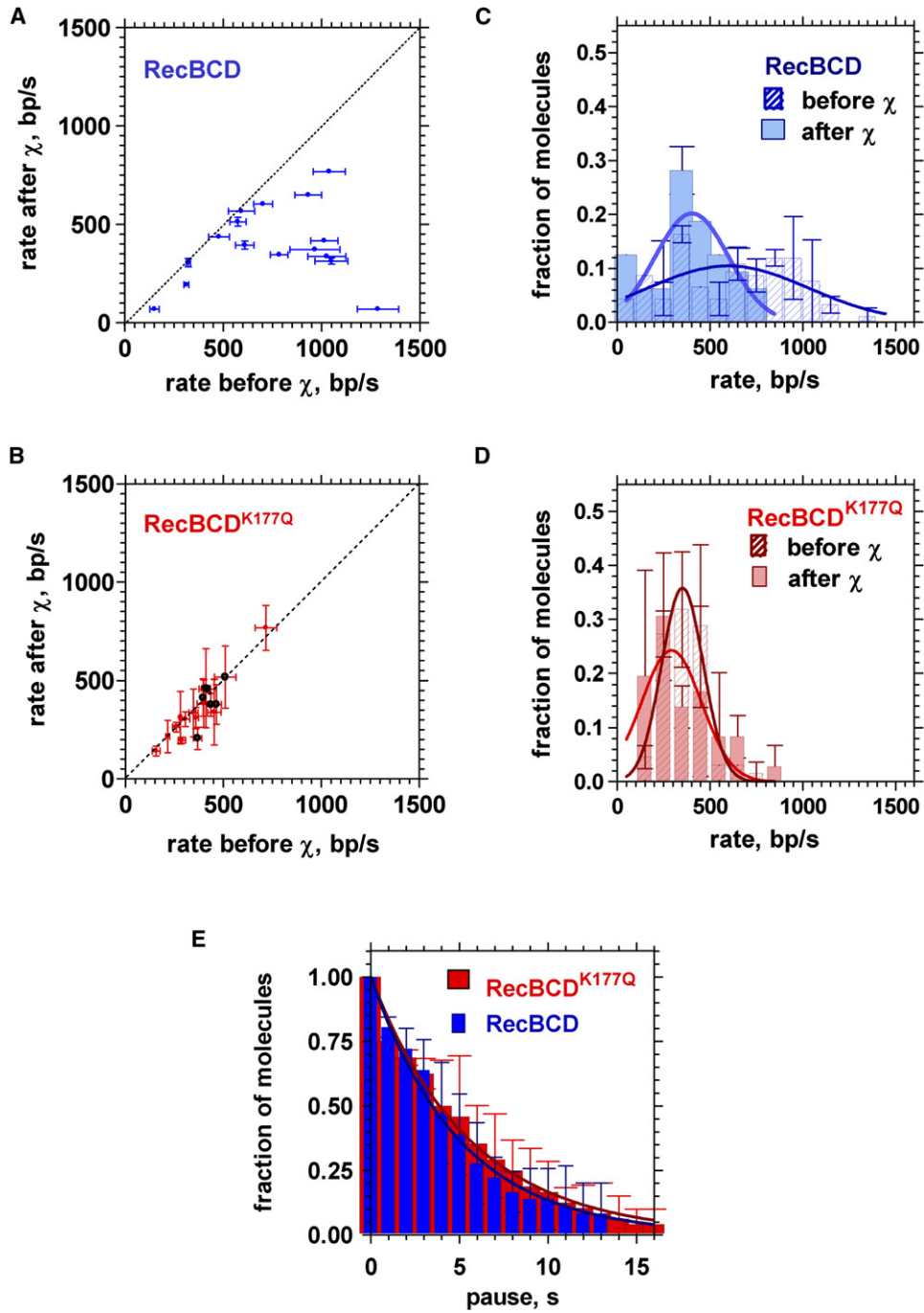


**Figure 3. RecBCD<sup>K177Q</sup> Translocates at the Same Velocity Both before and after  $\chi$  Recognition**

(A and B) Dot plot for the rate of DNA translocation prior to  $\chi$  versus the rate of translocation after  $\chi$ . The diagonal dotted line denotes the behavior expected if the rates were identical both before and after  $\chi$  recognition. For (A) and (B), the error bars represent one standard deviation from least-squares fitting; in the cases where the error bars are not visible, they are smaller than the size of the symbol used for the data point.

(A) For the individual wild-type enzymes, within experimental error, all molecules showed a reduced translocation rate after  $\chi$  recognition; also, there was no correlation between rates before and after  $\chi$  recognition. The errors for the rates before  $\chi$  are generally larger than for the rate after  $\chi$  because more data points are used to define the rates after  $\chi$  because of the greater distances traveled beyond  $\chi$  by the wild-type enzyme (see Figure 2). (B) For RecBCD<sup>K177Q</sup>, within experimental error, there was no change in the DNA translocation rate after pausing at  $\chi$ . Red symbols represent data obtained in the absence of P1 nuclease; black symbols represent data obtained in the presence of P1 nuclease.

(C and D) Distribution of the translocation velocities before and after interaction with  $\chi$  for RecBCD (C) and RecBCD<sup>K177Q</sup> (D). The rates were grouped in 100 bp/s bins; error bars represent the minimum and maximum boundaries of the observed rates obtained from the least-squares fit.

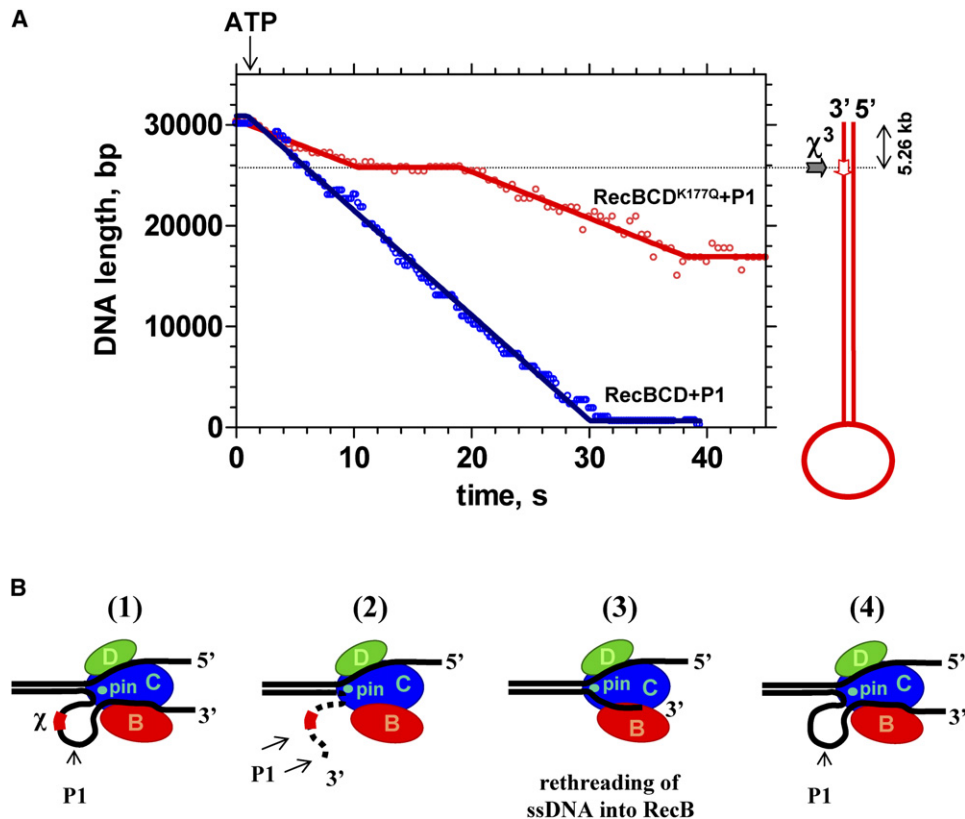


**Figure 4. The ssDNA-Specific Nuclease, P1, Eliminates  $\chi$  Recognition by the Wild-Type RecBCD, but Not by the RecBCD<sup>K177Q</sup> Mutant**

(A) Representative time courses for unwinding of a single  $\chi$ -containing DNA molecule in the presence of P1 nuclease. The DNA substrate is shown schematically on the right. The length of each DNA molecules was measured and is plotted as a function of time for RecBCD (blue circles) and RecBCD<sup>K177Q</sup> (red circles). The rates of DNA unwinding and both the duration and the position of the pause were determined by fitting the data to a continuous 5 segment line (the fitted lines for wild-type and mutant are shown in blue and red, respectively).

(B) Cartoon illustrating how, in case of the uncoupled translocation, fast translocation by the leading RecD subunit results in accumulation of P1 nuclease-sensitive ssDNA on the 3'-terminated strand in front of RecB subunit. (1) The ssDNA loop formed due to unequal rates of translocation by RecD and RecB will eventually contain the  $\chi$  sequence; (2) this ssDNA loop is degraded by the endo- and exonucleolytic cleavage activity of P1 nuclease; (3) continuing translocation by the enzyme results in rethreading of the 3'-terminated strand into the RecB subunit; and (4) generation of a new loop, with degradation repeated.

a single active motor subunit, did not create a P1-susceptible DNA species in front of the RecB subunit.

## DISCUSSION

RecBCD has an unusual structural architecture for a DNA helicase, comprising two motor subunits with opposite translocation polarities (Dillingham et al., 2003; Taylor and Smith, 2003). Furthermore, translocation by RecBCD is regulated by interaction with the recombination hotspot,  $\chi$ , adding to the list of enzymatic functions that are controlled by  $\chi$ . Here, we established that  $\chi$  regulates RecBCD translocation by a novel mechanism:  $\chi$  recogni-

tion elicits a switch in lead motor subunit usage. We confirmed that RecD is the lead, or faster (Taylor and Smith, 2003), subunit prior to  $\chi$ ; however, after  $\chi$  recognition, we discovered that this responsibility is switched to the RecB motor subunit. Thus, prior to  $\chi$ , RecD acts as the helicase subunit that unwinds the dsDNA, and RecB is simply a translocase that moves behind. However, after  $\chi$ , RecB becomes the helicase subunit; the functional fate of RecD is unknown, but it does remain associated with the holoenzyme (Handa et al., 2005). The capacity of each motor subunit to function as an autonomous processive helicase, within the RecBCD heterotrimer, is fully consistent with the biochemical behavior of the

(E) Distribution of the length of time that RecBCD and RecBCD<sup>K177Q</sup> pause at  $\chi$ . For each molecule that unwound DNA past  $\chi$ , the duration of the pause was obtained from a least-squares fit of the data to a multisegment line, and the error bars represent the longest and shortest boundaries of pause time determined with the standard deviations for the fitted line. The molecules that paused for at least the time indicated were grouped in 1 s bins. The pause times for wild-type and mutant decay exponentially with the half-times of  $3.5 \pm 0.3$  s and  $3.9 \pm 0.2$  s, respectively.

single-motor mutant enzymes (Dillingham et al., 2005; Spies et al., 2005; Taylor and Smith, 2003).

Our characterization of translocation by the mutant RecBCD<sup>K177Q</sup>, where RecB is the only functional motor, showed that it retains the ability to pause at  $\chi$ , but it does not alter its velocity after recognizing  $\chi$ . This simple observation permits two important conclusions. The first is that the pause at  $\chi$  cannot be explained simply as the difference in time required for the two uncoupled motor subunits to translocate to  $\chi$ ; rather, the pause measures the dwell time of RecBCD at  $\chi$ , which likely represents the time required for the conformational transition induced by  $\chi$  recognition needed to recommence translocation in the  $\chi$ -modified form. In addition, we can conclude that this dwell time is unrelated to the relative translocation velocities of the two motor subunits and, instead, reflects only an intrinsic lifetime of the RecBCD- $\chi$  recognition event. This conclusion follows most easily from the fact that the distribution of pause times is the same for both wild-type and the single-motor mutant (Figure 3E).

The second important conclusion that emerges from our study of the mutant RecBCD<sup>K177Q</sup> is that the change in translocation velocity does, however, require two functioning motor subunits. Given that the average translocation velocity of the RecBCD<sup>K177Q</sup> mutant is approximately 2-fold lower than the average velocity of the wild-type enzyme before  $\chi$  and, notably, is similar to the average velocity of the wild-type enzyme after  $\chi$ , we conclude that the RecB motor subunit is driving DNA unwinding after  $\chi$ .

Our real-time single-molecule experiments with P1 nuclease show unequivocally that a loop of ssDNA is generated prior to  $\chi$ , in complete agreement with earlier electron microscopic analysis of unwinding intermediates (Braedt and Smith, 1989; Muskavitch and Linn, 1982; Taylor and Smith, 1980, 2003). Furthermore, because P1 nuclease eliminated the normal  $\chi$ -dependent responses, we could conclude that the ssDNA loop is being generated on the  $\chi$ -containing DNA strand. This result means that the RecD subunit is the lead motor of RecBCD prior to  $\chi$  and that the RecB is translocating more slowly. Collectively, our data show that the  $\chi$ -induced modification of RecBCD involves switching the designation of the lead motor subunit (Figure 5).

Our experiments cannot determine the size of the ssDNA loop between RecD and RecB: we can only say that the amount of ssDNA revealed is sufficient for P1 endonucleolytic cleavage. The active site of P1 nuclease contains a proposed ssDNA binding tunnel about 20 Å in length connecting two nucleotide-binding pockets (Romier et al., 1998). Therefore, an ssDNA loop of seven nucleotides should be sufficient for cleavage by P1 nuclease. Although carried out under different conditions, electron microscopy showed that when DNA unwinding occurred at ~370 bp/s, loop growth occurred at ~150 nucleotides/s; from these values, we can infer that RecB was translocating at 220 nucleotides/s (Taylor and Smith, 2003). If both subunits were moving at the same relative rates in our experiments, this approximately 1.7-fold dif-

ference would have created a loop of about 2000 nucleotides when the RecD subunit reached  $\chi$  in our substrate (Figure 2). However, because the translocation velocities of the individual motors are sensitive to solution conditions (Spies et al., 2005), their relative velocities may differ from those quantified in the electron microscopic study, and the resulting loop size could be very different. In fact, other published ensemble experiments, described in the next paragraph, suggest that the loop size is considerably smaller.

An explicit feature of the uncoupled translocation model suggests that RecBCD pauses at the moment when RecB delivers the  $\chi$  sequence to the recognition site in RecC: i.e., the holoenzyme pauses by virtue of a conformational signal transmitted from RecC to RecD and, presumably, to RecB when RecB and RecC are at  $\chi$  (Figure 5). But because RecD is a faster motor subunit than RecB, this means that RecD will be *beyond*  $\chi$  when RecBCD pauses at the  $\chi$  sequence. Because the signal in our single-molecule experiments arises from YOYO-1 displacement, we should see RecBCD pausing not exactly at  $\chi$ , but downstream of it. Unfortunately, the typical uncertainty of 500–1000 bp in our measurements does not afford the precision needed to make this distinction. However, previous ensemble measurements are consistent with this model. When  $\chi$ -containing dsDNA is processed by RecBCD, recognition of  $\chi$  results in both attenuation of nuclease activity and a switch in polarity of nuclease activity (Anderson and Kowalczykowski, 1997a; Dixon and Kowalczykowski, 1993). As a consequence, two  $\chi$ -specific ssDNA fragments are produced: the downstream  $\chi$ -containing fragment and an upstream fragment derived from the complementary ssDNA. Although degradation of the  $\chi$ -containing 3'-terminated strand is downregulated precisely at  $\chi$  (Taylor and Smith, 1995), cleavage of the 5'-terminated (non- $\chi$ -containing) DNA strand occurs approximately 300–500 nucleotides *downstream* of the  $\chi$  complement (Anderson and Kowalczykowski, 1997a). This observation is consistent with the interpretation that, for this  $\chi$  location that was approximately 3 kb from the entry site, RecD is 300–500 bp ahead of RecB when the holoenzyme recognizes  $\chi$ : i.e., the loop size is 300–500 bp. The pause at  $\chi$  results in a high probability of cleaving both DNA strands in this loop-tailed configuration, resulting in the observed  $\chi$ -specific ssDNA fragments. Furthermore, in agreement with the other biochemical studies that suggested that the relative translocation velocities of the motor subunits are sensitive to solution conditions, the exact cleavage location on this  $\chi$ -complement-containing strand was sensitive to the free Mg<sup>2+</sup> ion concentration: at the highest tested free Mg<sup>2+</sup> ion concentration (8 mM Mg<sup>2+</sup>/1 mM ATP), the 5'-terminated strand was cleaved at the  $\chi$  sequence (within 100 bp accuracy) (Anderson et al., 1997), suggesting that the loop size is small at this reaction condition. We note that the unwinding velocity of RecB increases with increasing free Mg<sup>2+</sup> ion concentration (Spies et al., 2005). Thus, our model and observations are fully consistent with our

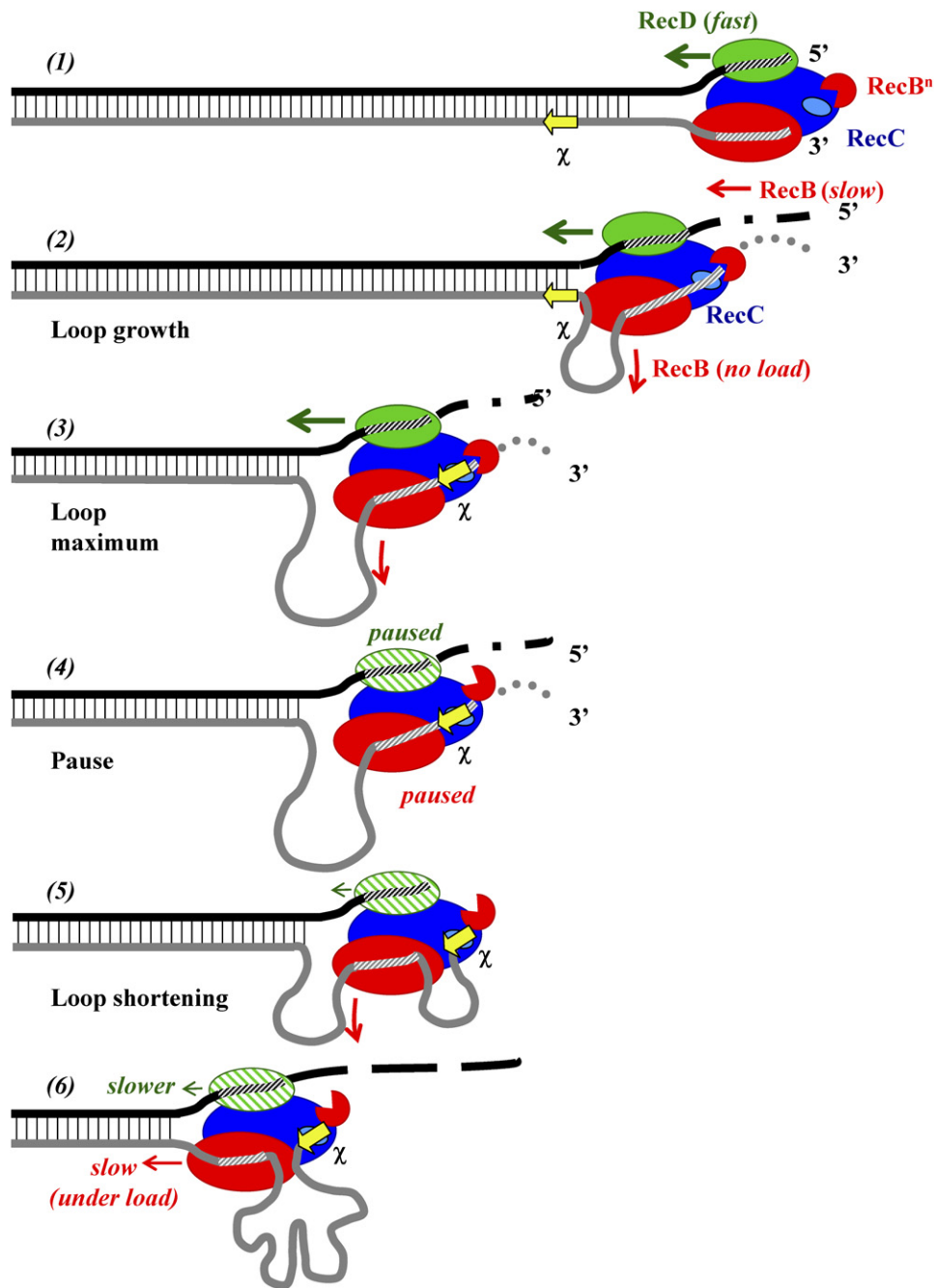


**Figure 5. Model Illustrating Uncoupled Translocation by the Two Motor Subunits of RecBCD, and the Consequences of  $\chi$  Recognition**

See text for details. RecBCD is shown as a bipolar helicase with its two motor subunits translocating on the opposite strands of the DNA molecule. Before  $\chi$ , the RecD subunit is shown as the leading motor subunit. Such an arrangement of the two motor subunits moving with different rates generates an ssDNA loop in front of the RecB subunit. Upon  $\chi$  recognition, the RecD motor is controlled and the RecB subunit becomes the driving motor of the enzyme. Arrows indicate the directions and relative rates of translocation by the motor subunits.

discussion in the preceding paragraph and with past findings.

Notably, P1 nuclease did not interfere with the processivity of wild-type enzyme, even though it nucleolytically uncoupled the translocation of RecB from RecD. Our pre-

vious studies argued that neither of the individual motor subunits can support translocation that is as rapid and as processive as observed for the dual-motor holoenzyme (Dillingham et al., 2005; Spies et al., 2005). This means that DNA unwinding by a solitary, faster RecD subunit cannot



explain the high translocation rate and processivity of RecBCD. Furthermore, the high processivity in the presence of P1 nuclease (see Figure 4) implies that, after the ssDNA loop formed between two subunits is digested by the nuclease, the 3'-terminated strand of the DNA duplex can be rethreaded into the active site of RecB subunit (Figure 4B). Although our current work does not further address this issue, this finding is not completely unexpected because the RecBC enzyme can step across ssDNA gaps of 22 nucleotides on the 3'-terminated strand and re-engage this discontinuous strand across the gap to continue unwinding (Bianco and Kowalczykowski, 2000). Also, the fact that  $\chi$ -modified wild-type enzyme is significantly more processive than RecBCD<sup>K177Q</sup> mutant implies that, whereas RecB subunit becomes drive motor after  $\chi$ , the RecD motor is not completely inactivated upon  $\chi$  recognition and still contributes to processive translocation (Table 1). This view is consistent with previous single-molecule work showing that the RecD subunit remains associated with the  $\chi$ -modified RecBCD (Handa et al., 2005). Thus, our current data suggest that RecD contributes to the processive translocation of RecBCD both before and after  $\chi$ .

The structure of RecBCD bound to dsDNA (Singleton et al., 2004) reveals the presence of tunnels for each of the DNA strands after they are separated by a pin structure in the RecC subunit (see Figure 1A). The 5'-terminated strand passes through the translocation site of the RecD subunit, whereas the  $\chi$ -containing 3'-terminated strand first passes through the translocation site of the RecB motor. This strand is then channeled through the enzyme to the  $\chi$ -recognition site residing in the RecC subunit. Afterward, the strands exit the enzyme in proximity to the active site of the nuclease domain located in the C terminus of the RecB subunit. Because the channel for the 3'-terminated ssDNA is enclosed within the core of the enzyme, the RecB motor must actively translocate the  $\chi$ -containing DNA strand through the channel to the  $\chi$ -recognition site. The ssDNA loop formed in front of the slower RecB subunit will contain the  $\chi$  sequence at some point during translocation. Eventually, the  $\chi$  sequence is translocated into the  $\chi$ -recognition site. We proposed that  $\chi$  sequence binds to the RecBCD holoenzyme and serves as the allosteric effector, which triggers a number of conformational changes in the enzyme (Kulkarni and Julin, 2004; Singleton et al., 2004; Spies et al., 2003; Spies and Kowalczykowski, 2006). One consequence of this conformational change is a switch in the drive motor of the enzyme—an unprecedented phenomenon for nucleic acid motor proteins.

Considering the aforementioned discussions, our current model for RecBCD function and its control by  $\chi$  includes elements from previous models and the discoveries reported here (Figure 5). In agreement with the “uncoupled translocation” model (Figure 1A), the RecD motor is responsible for the fast and processive translocation of the enzyme before  $\chi$ , resulting in a loop of ssDNA being formed in front of the RecB subunit (Figure 5,

steps 1 and 2; Taylor and Smith, 2003). The size of the loop and its rate of growth will depend on the velocity of RecB translocation relative to that of RecD translocation. The differential sensitivity of these motor subunits to solution conditions can create loops as large as thousands of nucleotides (Taylor and Smith, 1980, 2003), to inferred sizes of hundreds of nucleotides, or as little as tens of nucleotides (Anderson et al., 1997; Anderson and Kowalczykowski, 1997a). For the solution conditions employed here, which are approximately physiological in ATP and Mg<sup>2+</sup> concentration, several lines of evidence suggest that the ssDNA loop is small. First, the duration of pauses are the same for the wild-type and mutant enzymes, which would not be the expected result if RecB needed to travel a long distance to catch up to RecD after the  $\chi$ -induced pause. Second, as discussed, the loop must be smaller than the resolution of the single-molecule distance measurement (i.e., it must be less than ~1000 bp) because the pause occurs at  $\chi$ , within experimental error (Spies et al., 2003). Third, we have not seen evidence of ssDNA prior to  $\chi$  recognition in our single-molecule experiments, which would be expected if there was a significant amount of ssDNA formed before encountering the nuclease domain in RecB (Figure 5, step 3; Bianco et al., 2001; Spies et al., 2003). Finally, the position of the  $\chi$ -induced cleavage on the strand complementary to the  $\chi$  sequence is consistent with loop that would range from less than 100 nucleotide to at most 500 nucleotides (Anderson et al., 1997; Anderson and Kowalczykowski, 1997a). Although it is evident that the size of this “pre- $\chi$ ” ssDNA loop can be regulated, the precise control of its size is yet to be defined. However, the size of this loop may be less important than the fact that its existence means that the unwound ssDNA strands are not in complementary register when they exit RecBCD. Thus, spontaneous annealing will be minimized, and the probability of endonucleolytic cleavage by RecBCD will be maximized. Thus, one simple explanation for the function of the pre- $\chi$  loop is to enhance endonucleolytic degradation of the ssDNA produced prior to  $\chi$  recognition by preventing spontaneous renaturation of DNA strands behind RecBCD.

RecBCD stochastically cleaves the unwound 3'-terminated DNA strand endonucleolytically and, less frequently so, the 5'-terminated strand until  $\chi$  is recognized (Figure 5, step 3; Dixon and Kowalczykowski, 1993, 1995). At this moment, the enzyme pauses at  $\chi$ , which ensures that there is a high probability of a cleavage event at the  $\chi$  sequence; then, the nuclease activity is attenuated overall and switched to the 5'-terminated strand (Figure 5, step 4). At this time, the loop formed prior to  $\chi$  recognition will have reached its maximum size (Figure 5, step 4). But the realization is that, depending on the relative velocities of the motor subunits, the paused position for each subunit will be at a different location on each DNA strand. The model shows that the RecB subunit will be paused at the  $\chi$  sequence but that the RecD subunit will be paused on the opposite strand some distance downstream of the  $\chi$  complement; this distance will depend on the size

of ssDNA loop, which, in turn, will depend on the relative translocation velocities of the motor subunits. The model is fully consistent with biochemical identification of the “last” cleavage event on the  $\chi$ -containing strand being at  $\chi$  (from 0 to 6 nucleotides upstream of  $\chi$ , depending on solution conditions) (Dixon and Kowalczykowski, 1993, 1995; Ponticelli et al., 1985; Taylor et al., 1985; Taylor and Smith, 1995) and the “first” cleavage after the polarity switch on the complementary strand being at or several hundred nucleotides downstream of the  $\chi$ -complement sequence (Anderson et al., 1997; Anderson and Kowalczykowski, 1997a). Binding of the  $\chi$  sequence to the RecC subunit serves as a *cis*-acting allosteric modifier of RecBCD structure (Chédin et al., 2006; Handa et al., 2005; Singleton et al., 2004; Spies et al., 2003). As a consequence of this structural change, the speed of the RecD motor is attenuated to be equal to or below that of the RecB motor, but the change does not involve ejection of the RecD motor from the holoenzyme at  $\chi$  (Handa et al., 2005). We suggest that the pause is a measure of the kinetic lifetime required for this conformational change: as part of this change, the nuclease domain of RecB is proposed to undock from RecC, both revealing the cryptic RecA-loading site (Spies and Kowalczykowski, 2006) and altering the polarity of DNA degradation (Singleton et al., 2004; Yu et al., 1998).

After the pause at  $\chi$ , DNA unwinding resumes, but the  $\chi$ -modified RecBCD is functionally different (Figure 5, step 5). The 5'-terminated strand is now cleaved more frequently than the 3'-terminated strand, but the nuclease activity is attenuated overall (Figure 5, step 6; Anderson and Kowalczykowski, 1997a). RecB resumes translocation, and the existing loop between RecB and RecD shortens as RecB takes up the ssDNA “slack” (Figure 5, step 5). The  $\chi$  sequence remains bound to the RecC subunit of RecBCD, and therefore, after  $\chi$ , a new ssDNA loop between the  $\chi$  sequence bound to RecC and the translocating RecB forms and grows with distance traveled (Spies et al., 2003). The RecB motor now assumes the responsibility for DNA unwinding, and RecD serves an ancillary role that contributes to the enzymes processivity (Dillingham et al., 2005; Spies et al., 2005). The speed of RecD translocation relative to RecB is unknown at this time; however, if the two speeds are identical, then only the single ssDNA loop shown, involving the  $\chi$ -containing 3'-terminated DNA strand, would form; but if the speed of RecD were slower than that of RecB, then a second loop would form after  $\chi$  between the RecB and RecD subunits on the opposite 5'-terminated strand (not illustrated). This “post- $\chi$ ” ssDNA loop (or loops) is likely a component of the conformational changes in RecBCD that are elicited by  $\chi$  recognition (Spies et al., 2003; Spies and Kowalczykowski, 2006). Upon  $\chi$  recognition, the  $\chi$ -containing ssDNA may begin to exit through an alternative egress that is created between the RecB and RecC subunits (Singleton et al., 2004). Minimally, by having the ssDNA extrude through this new exit, the switched state of RecBCD is effectively locked until dissociation; further-

more, it is possible that the location of this exit facilitates the loading of RecA by positioning the  $\chi$ -containing ssDNA near the RecA-loading domain of the RecB subunit. This change in behavior enables the RecB subunit to begin loading RecA onto the  $\chi$ -containing ssDNA (not illustrated), thereby allowing the next step of recombinational DNA repair, which is homologous pairing, to ensue (Anderson and Kowalczykowski, 1997b; Spies and Kowalczykowski, 2006). Upon dissociating from the DNA, the subunits disassemble (Taylor and Smith, 1999), the  $\chi$  sequence dissociates, and the subunits reassemble to produce the unmodified RecBCD holoenzyme.

The specific biological reason for this complicated control of helicase subunit utilization and speed is largely unknown, but we offer the following observations and speculations. RecBCD clearly has two seemingly contradictory biological functions: the destruction of foreign (e.g., phage) DNA and the repair of chromosomal DNA upon  $\chi$  recognition. Destruction of foreign dsDNA would be optimal with a fast helicase coupled to rapid nucleolytic degradation, whereas repair of chromosomal DNA apparently requires a slower helicase whose speed is functionally matched to the relatively slow downstream process of RecA nucleoprotein filament assembly. Assembly of a RecA nucleoprotein filament is limited by its nucleation frequency (Gallego et al., 2006), a step that is facilitated by the  $\chi$ -activated RecBCD. Furthermore, because RecBCD must repeatedly nucleate RecA filaments for distances as far as 10 Kb downstream of  $\chi$  (Myers et al., 1995), the translocation velocity of RecBCD must be coordinated to the rates of RecA nucleoprotein filament nucleation and growth. Thus, it appears that the slower translocation of the  $\chi$ -modified RecBCD is a biological requirement of efficient RecA nucleoprotein filament formation. Furthermore, it is well established that RecBC, lacking the RecD subunit, is fully proficient for recombinational DNA repair (Amundsen et al., 1986). RecBC does not require  $\chi$  for activation, being constitutively activated for RecA loading (Churchill et al., 1999). However, RecBC does not destroy phage DNA (Chaudhury and Smith, 1984), suggesting that this simple single-motor enzyme, with little nucleolytic capacity, cannot fulfill the requisite protective function of RecBCD. Although it would seem that a “faster” version of RecBC, in conjunction with other cellular nucleases, could provide this degradative function, it appears instead that RecBC acquired another motor subunit to provide both a faster rate of helicase activity and another means of controlling nuclease activity. Thus, by using the faster dual motor RecBCD that is also activated for nuclease activity, destruction of foreign DNA is assured. However, through its interaction with a  $\chi$  sequence, both the helicase and nuclease activity of RecBCD can be regulated to switch the enzyme between two seemingly contradictory biological behaviors: the fast, degradative helicase/nuclease and the slower, DNA-repairing mobile RecA loader. Thus, we suggest that the biological function of this motor switch at  $\chi$  is to coordinate the speed of RecBCD translocation with the loading of RecA onto the

$\chi$ -containing ssDNA. The slower speed would facilitate a frequency of RecA nucleation onto the  $\chi$ -containing ssDNA that is sufficiently recurrent to ensure the discontinuous assembly of the RecA nucleoprotein filament over distances of 10 kb, an assembly that is essential to complete the recombinational repair of broken chromosomal DNA.

## EXPERIMENTAL PROCEDURES

### Proteins and DNA Substrates

RecBCD and RecBCD<sup>K177Q</sup> were purified by published protocols (Dillingham et al., 2003; Roman and Kowalczykowski, 1989). P1 nuclease was from Roche.

Chi-containing dsDNA substrates were produced as described previously (Spies et al., 2003) with minor modifications. Biotinylated dsDNA was produced by amplification of a 30 kb region of  $\chi$ -containing  $\lambda$  DNA purified with the Lambda Purification Kit from QIAGEN (Spies et al., 2003). EXL polymerase (Stratagene) and a biotinylated (5'-bio-AGTATCGGTAAGGCGGTGAC-3') and a nonbiotinylated (5'-GCCCATGACAGGAAGTTGTT-3') primer were used for the PCR reaction. The PCR product was 30,870 bp in length and contained a  $\chi$ -recognition locus (three consecutive  $\chi$  sequences spaced 10 nucleotides apart) at 5.26 kb from the nonbiotinylated end. Full-length dsDNA was separated from shorter PCR products by electrophoresis in 0.8% agarose and electro-elution with Gene Capsule DNA extraction kit (Genotech).

### DNA Bead Preparation

The protocol for DNA bead preparation was modified from Spies et al. (2003). The biotinylated DNA (~25 ng at ~1 ng/ $\mu$ l) was incubated with 5  $\mu$ l of 1  $\mu$ m, "ProActive" streptavidin-coated microspheres (Bangs Laboratories) for 1 hr on ice in 80 mM NaHCO<sub>3</sub> (pH 8.2). Bead-DNA complexes were transferred into 1.5 ml of degassed "sample solution" containing 45 mM NaHCO<sub>3</sub> (pH 8.2), 20% (w/v) sucrose, 50 mM DTT, and 100 nM YOYO-1 (Molecular Probes). Immediately before transfer to the sample syringe, 2 mM magnesium acetate and 50 nM wild-type or mutant RecBCD enzymes were added. The reaction solution contained 45 mM NaHCO<sub>3</sub> (pH 8.2), 20% (w/v) sucrose, 50 mM DTT, 1 mM ATP, 2 mM magnesium acetate, and 20 nM YOYO-1. When indicated, P1 nuclease was added to the reaction solution to a final concentration of 25 units/ml.

### Optical Trapping and Fluorescence Microscopy

Reactions were performed as described (Bianco et al., 2001; Spies et al., 2003) but with the following modifications. A new instrument included a Nikon TE2000-U inverted microscope, YOYO-1 was excited with a 488 nm laser, and two neutral density filters combined with highest sensitivity settings on camera were used to ensure maximum fluorescence with minimum photobleaching.

### Data Analysis

Videos of the enzyme translocation were recorded at 10 frames per second with Scion Image Software. Every 5 frames were averaged with an ImageJ plug-in to reduce background and create 2 frames/s movies. The length of the DNA molecule in each frame was measured with a plug-in written in this laboratory (B. Liu and S.C.K., unpublished). The rates before and after  $\chi$ , as well as position and duration of the pause, were determined by fitting experimental data to a contiguous five-segment line with GraphPad Prism Software.

### Supplemental Data

Four tables are available at <http://www.cell.com/cgi/content/full/131/4/694/DC1/>.

## ACKNOWLEDGMENTS

We are grateful to Clarke Conant, Petr Cejka, Mark Dillingham, Anthony Forget, Jovencio Hilario, Ryan Jensen, Bian Liu, Edgar Valencia-Morales, Jody Plank, Behzad Rad, and Jason Wong; to the members of Spies lab for their critical reading of the manuscript; and to Martin Singleton for the structure of RecBCD in Figure 1. This work was supported by National Institutes of Health grant GM-41347 to S.C.K. and by American Cancer Society Postdoctoral Fellowship PF-02-116-01-GMC to M.S.

Received: May 19, 2007

Revised: August 28, 2007

Accepted: September 13, 2007

Published: November 15, 2007

## REFERENCES

- Amundsen, S.K., Taylor, A.F., Chaudhury, A.M., and Smith, G.R. (1986). *recD*: the gene for an essential third subunit of exonuclease V. *Proc. Natl. Acad. Sci. USA* **83**, 5558–5562.
- Anderson, D.G., and Kowalczykowski, S.C. (1997a). The recombination hot spot  $\chi$  is a regulatory element that switches the polarity of DNA degradation by the RecBCD enzyme. *Genes Dev.* **11**, 571–581.
- Anderson, D.G., and Kowalczykowski, S.C. (1997b). The translocating RecBCD enzyme stimulates recombination by directing RecA protein onto ssDNA in a  $\chi$ -regulated manner. *Cell* **90**, 77–86.
- Anderson, D.G., Churchill, J.J., and Kowalczykowski, S.C. (1997). Chi-activated RecBCD enzyme possesses 5'  $\rightarrow$  3' nucleolytic activity, but RecBC enzyme does not: evidence suggesting that the alteration induced by Chi is not simply ejection of the RecD subunit. *Genes Cells* **2**, 117–128.
- Bianco, P.R., and Kowalczykowski, S.C. (2000). Translocation step size and mechanism of the RecBC DNA helicase. *Nature* **405**, 368–372.
- Bianco, P.R., Brewer, L.R., Corzett, M., Balhorn, R., Yeh, Y., Kowalczykowski, S.C., and Baskin, R.J. (2001). Processive translocation and DNA unwinding by individual RecBCD enzyme molecules. *Nature* **409**, 374–378.
- Braedt, G., and Smith, G.R. (1989). Strand specificity of DNA unwinding by RecBCD enzyme. *Proc. Natl. Acad. Sci. USA* **86**, 871–875.
- Chaudhury, A.M., and Smith, G.R. (1984). A new class of *Escherichia coli recBC* mutants: implications for the role of RecBC enzyme in homologous recombination. *Proc. Natl. Acad. Sci. USA* **81**, 7850–7854.
- Chédin, F., Handa, N., Dillingham, M.S., and Kowalczykowski, S.C. (2006). The AddAB helicase/nuclease forms a stable complex with its cognate  $\chi$  sequence during translocation. *J. Biol. Chem.* **281**, 18610–18617.
- Churchill, J.J., Anderson, D.G., and Kowalczykowski, S.C. (1999). The RecBC enzyme loads RecA protein onto ssDNA asymmetrically and independently of Chi, resulting in constitutive recombination activation. *Genes Dev.* **13**, 901–911.
- Dillingham, M.S., Spies, M., and Kowalczykowski, S.C. (2003). RecBCD enzyme is a bipolar DNA helicase. *Nature* **423**, 893–897.
- Dillingham, M.S., Webb, M.R., and Kowalczykowski, S.C. (2005). Bipolar DNA translocation contributes to highly processive DNA unwinding by RecBCD enzyme. *J. Biol. Chem.* **280**, 37069–37077.
- Dixon, D.A., and Kowalczykowski, S.C. (1991). Homologous pairing in vitro stimulated by the recombination hotspot, Chi. *Cell* **66**, 361–371.
- Dixon, D.A., and Kowalczykowski, S.C. (1993). The recombination hotspot  $\chi$  is a regulatory sequence that acts by attenuating the nuclease activity of the E. coli RecBCD enzyme. *Cell* **73**, 87–96.

- Dixon, D.A., and Kowalczykowski, S.C. (1995). Role of the *Escherichia coli* recombination hotspot,  $\chi$ , in RecABCD-dependent homologous pairing. *J. Biol. Chem.* *270*, 16360–16370.
- Galletto, R., Amitani, I., Baskin, R.J., and Kowalczykowski, S.C. (2006). Direct observation of individual RecA filaments assembling on single DNA molecules. *Nature* *443*, 875–878.
- Handa, N., Bianco, P.R., Baskin, R.J., and Kowalczykowski, S.C. (2005). Direct visualization of RecBCD movement reveals cotranslocation of the RecD motor after  $\chi$  recognition. *Mol. Cell* *17*, 745–750.
- Korangy, F., and Julin, D.A. (1992). Alteration by site-directed mutagenesis of the conserved lysine residue in the ATP-binding consensus sequence of the RecD subunit of the *Escherichia coli* RecBCD enzyme. *J. Biol. Chem.* *267*, 1727–1732.
- Kulkarni, A., and Julin, D.A. (2004). Specific inhibition of the *E. coli* RecBCD enzyme by Chi sequences in single-stranded oligodeoxyribonucleotides. *Nucleic Acids Res.* *32*, 3672–3682.
- Lam, S.T., Stahl, M.M., McMilin, K.D., and Stahl, F.W. (1974). Rec-mediated recombinational hot spot activity in bacteriophage lambda. II. A mutation which causes hot spot activity. *Genetics* *77*, 425–433.
- Muskavitch, K.M., and Linn, S. (1982). A unified mechanism for the nuclease and unwinding activities of the recBC enzyme of *Escherichia coli*. *J. Biol. Chem.* *257*, 2641–2648.
- Myers, R.S., Stahl, M.M., and Stahl, F.W. (1995). Chi recombination activity in phage lambda decays as a function of genetic distance. *Genetics* *141*, 805–812.
- Ponticelli, A.S., Schultz, D.W., Taylor, A.F., and Smith, G.R. (1985). Chi-dependent DNA strand cleavage by RecBC enzyme. *Cell* *41*, 145–151.
- Roman, L.J., and Kowalczykowski, S.C. (1989). Characterization of the helicase activity of the *Escherichia coli* RecBCD enzyme using a novel helicase assay. *Biochemistry* *28*, 2863–2873.
- Roman, L.J., Eggleston, A.K., and Kowalczykowski, S.C. (1992). Processivity of the DNA helicase activity of *Escherichia coli* recBCD enzyme. *J. Biol. Chem.* *267*, 4207–4214.
- Romier, C., Dominguez, R., Lahm, A., Dahl, O., and Suck, D. (1998). Recognition of single-stranded DNA by nuclease P1: high resolution crystal structures of complexes with substrate analogs. *Proteins* *32*, 414–424.
- Singleton, M.R., Dillingham, M.S., Gaudier, M., Kowalczykowski, S.C., and Wigley, D.B. (2004). Crystal structure of RecBCD enzyme reveals a machine for processing DNA breaks. *Nature* *432*, 187–193.
- Spies, M., and Kowalczykowski, S.C. (2005). Homologous recombination by RecBCD and RecF pathways. In *The Bacterial Chromosome*, N.P. Higgins, ed. (Washington, D.C.: ASM Press), pp. 389–403.
- Spies, M., and Kowalczykowski, S.C. (2006). The RecA binding locus of RecBCD is a general domain for recruitment of DNA strand exchange proteins. *Mol. Cell* *21*, 573–580.
- Spies, M., Bianco, P.R., Dillingham, M.S., Handa, N., Baskin, R.J., and Kowalczykowski, S.C. (2003). A molecular throttle: the recombination hotspot  $\chi$  controls DNA translocation by the RecBCD helicase. *Cell* *114*, 647–654.
- Spies, M., Dillingham, M.S., and Kowalczykowski, S.C. (2005). Translocation by the RecB motor is an absolute requirement for  $\chi$ -recognition and RecA protein loading by RecBCD enzyme. *J. Biol. Chem.* *280*, 37078–37087.
- Taylor, A., and Smith, G.R. (1980). Unwinding and rewinding of DNA by the RecBC enzyme. *Cell* *22*, 447–457.
- Taylor, A.F., and Smith, G.R. (1995). Strand specificity of nicking of DNA at Chi sites by RecBCD enzyme: modulation by ATP and magnesium levels. *J. Biol. Chem.* *270*, 24459–24467.
- Taylor, A.F., and Smith, G.R. (1999). Regulation of homologous recombination: Chi inactivates RecBCD enzyme by disassembly of the three subunits. *Genes Dev.* *13*, 890–900.
- Taylor, A.F., and Smith, G.R. (2003). RecBCD enzyme is a DNA helicase with fast and slow motors of opposite polarity. *Nature* *423*, 889–893.
- Taylor, A.F., Schultz, D.W., Ponticelli, A.S., and Smith, G.R. (1985). RecBC enzyme nicking at Chi sites during DNA unwinding: location and orientation-dependence of the cutting. *Cell* *41*, 153–163.
- Yu, M., Souaya, J., and Julin, D.A. (1998). The 30-kDa C-terminal domain of the RecB protein is critical for the nuclease activity, but not the helicase activity, of the RecBCD enzyme from *Escherichia coli*. *Proc. Natl. Acad. Sci. USA* *95*, 981–986.